Linkage between Fructose 1,6-Bisphosphate Binding and the Dimer−Tetramer Equilibrium of *Escherichia coli* Glycerol Kinase: Critical Behavior Arising from Change of Ligand Stoichiometry†

Peng Yu and Donald W. Pettigrew*

Department of Biochemistry and Biophysics, Center for Advanced Biomolecular Research, Texas A&M University, College Station, Texas 77843-2128

Received November 8, 2002; Revised Manuscript Received January 30, 2003

ABSTRACT: *Escherichia coli* glycerol kinase (EC 2.7.1.30; ATP−glycerol 3-phosphotransferase) is inhibited allosterically by fructose 1,6-bisphosphate (FBP), and this inhibition is a primary mechanism by which glucose controls glycerol utilization in vivo. Earlier work indicates that glycerol kinase displays a dimer−tetramer equilibrium in solution, FBP shifts the equilibrium toward the tetramer, and tetramer formation is required for FBP inhibition. However, equilibrium constants for FBP binding and dimer−tetramer assembly that describe the linkage between these processes are unknown. Here, decreased fluorescence anisotropy of extrinsic fluorophores fluorescein and 2′,7′-difluorofluorescein due to homo fluorescence resonance energy transfer (homo-FRET) is used to quantitate tetramer assembly and FBP binding. Glycerol kinase is labeled with extrinsic fluorophores covalently attached to an engineered surface cysteine residue under conditions that prevent labeling of native cysteine residues. Tryptic peptide mapping and MALDI-MS verify labeling at the engineered site only. Initial velocity studies show the labeling does not alter the catalytic properties or FBP inhibition. The steady-state fluorescence anisotropy of enzyme with a labeling stoichiometry of ∼0.1 mol of fluorophore/mol of subunit is not sensitive to increased protein concentration or binding of FBP, indicating the absence of homo-FRET. However, steady-state fluorescence anisotropy of enzyme with a labeling stoichiometry of ∼0.4 mol of fluorophore/mol of subunit decreases with increasing protein concentration, which is consistent with depolarization due to homo-FRET. The protein concentration dependence of the decreased fluorescence anisotropy is described by a dimer−tetramer equilibrium with an apparent dissociation constant of 61 ± 7 nM (subunits) at pH 7.0 and 25 °C. FBP binds to both the dimer and tetramer of glycerol kinase, and the FBP concentration dependence of the apparent dissociation constant for the dimer−tetramer equilibrium shows critical behavior. The apparent dissociation constant decreases and then increases with increasing FBP concentration, reaching a minimum at about 20 mM FBP. Critical behavior is seen also in the FBP dependence of the inhibition. The critical behavior arises because tetramer dissociation increases FBP stoichiometry from two sites per tetramer to four half-sites per two dimers. The phenomenological description of the coupling between tetramer assembly and FBP binding shows antagonistic binding of FBP to the two sites on the tetramer, indicating that the strong positive cooperativity observed for FBP inhibition of catalytic activity (Hill coefficient ∼1.5) is due to the ∼4000-fold higher affinity of the tetramer for FBP rather than to positive coupling between the two FBP sites.

Two unrelated bacterial enzyme families show FBP[1] allosteric control of catalysis and remarkable similarity of oligomeric structure and FBP binding: L-lactate dehydrogenase from several species (*1*−*5*) and glycerol kinase from *Escherichia coli* (*6*) and *Haemophilus influenzae* (*7*). In both families, FBP control is a key element of regulation of carbohydrate metabolism. FBP activation of lactate dehydrogenase controls partitioning of pyruvate between lactate and products of oxidative metabolism (*5*). Studies in vivo show that FBP inhibition of *E. coli* glycerol kinase is essential for glucose to prevent glycerol utilization during diauxic growth (*8*−*12*). Allosteric control by FBP displays nonclassical behavior in both enzyme families, decreasing both V_{max} and K_m. Crystal structures of the enzyme−FBP complexes of members of both families show that the enzymes are tetramers and FBP binds to two sites per tetramer, forming bridges between dimers with one-half of an FBP-binding site on each side of a tetramer interface, as shown in Figure 1 for *E. coli* glycerol kinase (*3*, *13*, *14*).

It is clear that tetramer formation is required for FBP control. Amino acid substitutions in the tetramer interface that contains the FBP-binding sites (S58 in interface 2 in

† Supported by grants from the National Institutes of Health (GM-49992) and the Robert A. Welch Foundation (A-1479) and by the Texas Agricultural Experiment Station (H-6559).

* To whom correspondence should be directed. E-mail: dpettigrew@tamu.edu.

[1] Abbreviations: FBP, fructose 1,6-bisphosphate; G3P, L-glycerol 3-phosphate; gol, glycerol; IIA^{Glc}, the glucose-specific phosphocarrier protein of the phosphoenolpyruvate:glycose phosphotransferase system; OG, Oregon Green 488 (2′,7′-difluorofluorescein); homo-FRET, homofluorescence resonance energy transfer; TEA, triethanolamine.

10.1021/bi027142l CCC: $25.00
Published on Web 03/20/2003

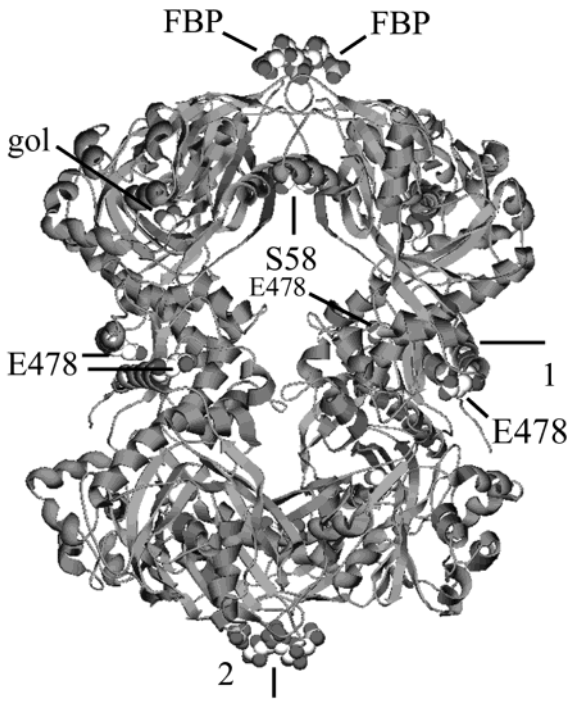

FIGURE 1: Structure of the *E. coli* glycerol kinase−FBP complex. The protein structure of the tetramer is shown as ribbons with FBP, glycerol (gol), and selected amino acid residues shown in space-filled representation. Occupied FBP-binding sites are shown at the top and bottom of the tetramer, and the two modes of binding at the upper binding site are indicated. The active site of one subunit is shown by the labeled glycerol. The amino acid residues S58 in the tetramer interface and E478 are shown as space-filled models, and lines show the E478 site in each subunit. The two possible interfaces for tetramer dissociation are indicated by the lines that are labeled with the numerals 1 and 2; dissociation along interface 2 yields the functional dimer described in the text. The two E478 residues on the left-hand side of the figure are contained in one functional dimer and are separated by ~50 Å. The E478 residues in each functional dimer are ~50 Å from those in the other dimer. The image was generated from Protein Data Bank file 1BO5 (*13*) by using the molecular graphics program SPOCK (*15*) to produce the tetramer from the file coordinates and Swiss-Pdb Viewer version 3.5 (*16*) to produce an image that was rendered by using POV-Ray for Windows version 3.1 (http://www.povray.org/).

Figure 1) interfere with tetramer formation and greatly reduce the apparent affinity for FBP for both enzyme families (*11*, *17*−*19*). However, quantitative relations between FBP binding, oligomeric state, and the physiologically important allosteric control of catalysis are not established for these enzymes. Here, we establish quantitatively the coupling between FBP binding and the oligomeric state for *E. coli* glycerol kinase.

Some aspects of the oligomeric structure of *E. coli* glycerol kinase and its relation to FBP binding have been described. Sedimentation equilibrium (*20*) and velocity (*7*) ultracentrifugation at a loading protein concentration of 3−5 μM (subunits) yield a molecular weight and sedimentation coefficient, respectively, of 217000 and 10.3 ± 0.1 S, which are the values expected for the tetramer (*21*). The same sedimentation coefficient is obtained with 0 and 5 mM FBP. Three methods were used to evaluate tetramer dissociation (*21*, *22*). Results of sucrose density gradient centrifugation, small-zone analytical gel permeation chromatography, and fitting the kinetics of sensitization and desensitization to FBP inhibition are consistent with a dimer−tetramer equilibrium which is shifted toward the tetramer by FBP binding. No evidence for dissociation of dimers to monomers or aggregation of tetramers was obtained over a wide range of protein concentrations. However, the value of the dimer−tetramer dissociation constant that was determined from sucrose density gradient centrifugation differs by more than 1000-fold from those determined by the other two methods, which show good agreement. Variants of *E. coli* glycerol kinase with the amino acid substitution S58W or A65T abolish FBP inhibition in solution (*17*, *18*).[2] The sites of these substitutions are located in the same tetramer interface as the FBP-binding sites, as seen in Figure 1. Small-zone analytical gel permeation chromatography shows that each of these enzymes in solution has the molecular size corresponding to a dimer in the absence and presence of FBP. Results of these earlier studies strongly support the conclusions that (1) *E. coli* glycerol kinase displays an FBP-sensitive dimer−tetramer equilibrium in solution and (2) tetramer dissociation occurs along the interface that contains the FBP-binding sites (interface 2 in Figure 1) to generate what we term the functional dimer (*23*). However, the affinities for FBP binding to the dimer and tetramer are unknown.

The linkage between FBP binding and the dimer−tetramer equilibrium of glycerol kinase is in some respects similar to the linkage between oxygen binding and the dimer−tetramer equilibrium of human hemoglobins. Linkage analysis of the ligand-coupled equilibrium of hemoglobins has provided powerful insights into allosteric control by homotropic interactions (*24*). The mode of FBP binding to *E. coli* glycerol kinase is analogous to binding of ATP to hemoglobins and has important ramifications for a linkage analysis (*25*). ATP binds to a single site per hemoglobin tetramer which yields two half-sites upon dissociation of the tetramer to dimers. Thus, the ligand binding stoichiometry doubles upon tetramer dissociation. An important consequence of the increased stoichiometry is observation of critical behavior in the dependence of the apparent tetramer dissociation constant on ATP concentration. That is, as the concentration of ATP is increased from zero, the apparent dissociation constant decreases and then increases, showing a minimum. Such behavior was observed by sedimentation velocity studies of ATP binding to human methemoglobin A (*25*).

Observation of the critical behavior requires that the ligand show measurable affinity for binding to the dimer at the half-site that results from dissociation such that the stoichiometry doubles upon dissociation. The novel binding of FBP to the tetramer of *E. coli* glycerol kinase strongly suggests this may be the case for this enzyme (*13*). Each of the two FBP-binding sites of the tetramer contains contributions from each dimer, and there are two modes of FBP binding at each of the sites. The two modes of FBP binding at each site in the tetramer, as seen in Figure 1, derive from the symmetry of the intersubunit FBP-binding sites at each end of the tetramer. The binding sites lie on a noncrystallographic 2-fold axis with the 6-phosphate group of the bound FBP lying on the 2-fold axis. This symmetry results in two mutually exclusive and equally populated FBP-binding modes in the crystal, for which the centrally positioned 6-phosphate is common.

[2] Glycerol kinase variants are denoted by single-letter amino acid abbreviations; e.g., E478C means that the native glutamate residue at position 478 is replaced by cysteine in the variant enzyme.

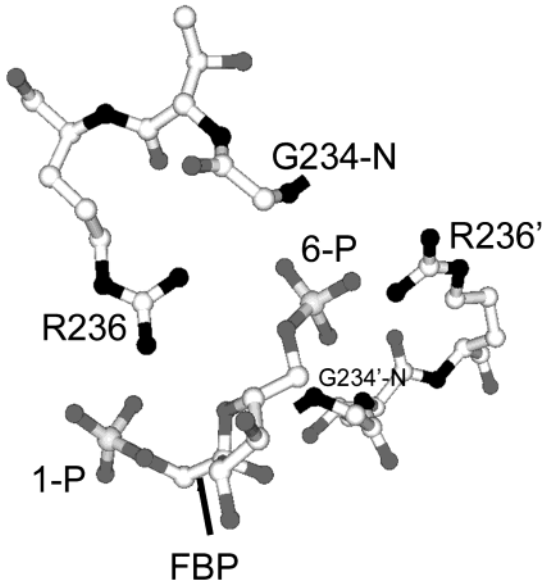

FIGURE 2: Structure of the tetramer FBP-binding site showing one mode of FBP binding. FBP bound in one of the two symmetry-related modes at the site formed by two subunits of the tetramer (see Figure 1) is indicated, and the 1-phosphate (1-P) and 6-phosphate (6-P) groups are labeled. The glycerol kinase amino acid residues G234 and R236 that form the binding site are shown, where the prime symbol indicates that the residue is from the other subunit. The binding site is formed by interactions of the guanidinium group of R236 and the amide hydrogen of G234 with the phosphate groups of FBP as shown.

Details of the binding interactions for one mode at one site are shown in Figure 2.

The binding site is composed of amino acid residues G234 and R236 from each subunit. In one subunit, the guanidinium group of R236 bridges the 1-phosphate and the 6-phosphate of FBP, and the amide hydrogen from G234 interacts with the 6-phosphate also. The 6-phosphate interacts also with G234 and R236 from the other subunit. For this FBP-binding mode, it is these latter interactions that are lost if the tetramer dissociates along this interface, leaving the former interactions intact. The R236 bridging interaction between the 1- and 6-phosphates and the interaction between G234 and the 6-phosphate would constitute the half-site. The converse case obtains for the other FBP-binding mode at this site, constituting the other half-site that is formed from this site. Upon tetramer dissociation, one-half of the binding site of each mode remains in a dimer, thus doubling the ligand binding stoichiometry. If FBP shows measurable affinity for this half-site, the resulting increase in ligand binding stoichiometry will result in critical behavior in the FBP concentration dependence of the dimer−tetramer dissociation.

Here, we show that critical behavior is observed in the FBP concentration dependence of both the allosteric inhibition of *E. coli* glycerol kinase and the apparent dissociation constant for the dimer−tetramer equilibrium, indicating that FBP binds to the dimer half-sites. The linkage relationships between FBP binding and the dimer−tetramer dissociation reaction in the absence of catalysis are quantitated by using fluorescence depolarization due to homo-FRET of an extrinsic fluorophore that is conjugated to an engineered surface cysteine residue.

MATERIALS AND METHODS

Materials. All chemicals were purchased from Sigma Chemical Co., St. Louis, MO, unless indicated otherwise. The E478C variant glycerol kinase was expressed and purified as described (*26*). Iodoacetamido derivatives of fluorescein and OG were purchased from Molecular Probes, Inc. (Eugene, OR), and used without further purification.

Labeling Glycerol Kinase with Fluorophores. Glycerol kinase was equilibrated by Sephadex G-25 chromatography with 0.1 M TEA, pH 7.0 or 8.0. Glycerol and ATP (2 mM final concentration) were added to the enzyme solution. A 5-fold molar excess of fluorophore (stock solution 6 mM in dimethyl sulfoxide) was added to initiate the reaction, and it was incubated for 1 h at room temperature in the dark. The reaction was quenched by adding a 100-fold molar excess of β-mercaptoethanol. Unreacted fluorophore and substrates were removed by Sephadex G-25 column chromatography at room temperature, followed by overnight dialysis at 4 °C against 1000 volumes of 0.1 M TEA, pH 7.0.

The glycerol kinase protein concentration was determined from absorbance at 280 nm by using the extinction coefficient 1.73 [mL/(mg cm)]. The stoichiometry of fluorescent label incorporation was determined from absorbance measurements at 280 nm and the wavelength of maximum absorbance of the fluorophore, using the equation and the extinction coefficients supplied by Molecular Probes, Inc.

Peptide Separation and Characterization. Glycerol kinase was denatured, carboxymethylated, and treated with trypsin as described (*27*). HPLC separation and MALDI-MS were performed by The Protein Chemistry Laboratory of Texas A&M University. For HPLC separation, the tryptic peptides were loaded onto a Vydac C18 reverse-phase column (2.1 × 150 mm). The column was developed with the eluent, starting from 0.05% trifluoroacetic acid in water with a gradient of 1% increment in solution B (0.04% trifluoroacetic acid in acetonitrile) per minute to separate peptides. Elution profiles were determined from absorbance at 214 and 490 nm simultaneously. The peptides of interest were collected manually and mixed 1:1 (v/v) with α-cyano-4-hydroxycinnamic acid (6 mg/mL in methanol). The mixture was spotted on a sample plate and run in linear mode on the MALDI-TOF instrument (Applied Biosystems Voyager). Spectra were obtained from averages of 128 laser shots.

Initial Velocity and FBP Inhibition Studies. Initial velocities at pH 7.0 and 25 °C were determined by using an ADP-coupled spectrophotometric assay with A_{340} measured on a Beckman DU640 spectrophotometer (*26*). The concentrations of ATP and glycerol were varied, and the reactions were initiated by the addition of glycerol kinase [3.6 nM (subunits)]. The initial velocity data were fitted by using the computer program Enzfitter to eq 1 for a sequential kinetic mechanism for the two-substrate enzyme, where v_0 is the initial velocity, K_{ATP} and K_{gol} are the Michaelis constants for ATP and glycerol, respectively, K_{iATP} is the dissociation constant for ATP, and V_{max} is the maximum reaction velocity:

$$v_0 = \frac{V_{max}[ATP][gol]}{[ATP][gol] + K_{ATP}[gol] + K_{gol}[ATP] + K_{iATP}K_{gol}} \quad (1)$$

Initial velocities are expressed as specific activity (units/mg), where one unit of glycerol kinase activity is the amount of enzyme that produces 1 μmol of ADP/min in this assay. FBP inhibition studies use the same assay with 0.2 mM ATP, 2 mM glycerol, 9 nM (subunits) glycerol kinase, and 15 different concentrations of FBP from 0 to 8 mM. The inhibition assays were incubated for 2 h at room temperature and then 5 min at 25 °C before initiation of the reaction by addition of ATP. Inhibition by FBP is given by the ratio of specific activity at a given concentration of FBP relative to the specific activity in the absence of FBP expressed as a percentage, and the data are fitted by using Kaleidagraph to eq 2 to obtain values for I_{max}, the maximum extent of inhibition; n_H, the Hill coefficient; and $K_{0.5}$, the apparent dissociation constant at half-maximal inhibition. By using these assay conditions, the critical behavior as a function of FBP concentration is not observed, and the data are well described by eq 2.

$$\text{SA}\ (\%) = 100 - \frac{100 I_{max}[\text{FBP}]^{n_H}}{[\text{FBP}]^{n_H} + K_{0.5}^{n_H}} \qquad (2)$$

Fluorescence Measurements. Emission spectra and steady-state anisotropy measurements were obtained by using an SLM 4800 spectrofluorometer equipped with Glan-Thompson calcite prism-type polarizers. All measurements are done at 25 °C. The excitation wavelength was 485 nm, and an OG 515 nm cut-on filter was used to collect the emission. The Raman scattering background was subtracted by using a blank of unlabeled E478C of the same concentration.

The steady-state anisotropy, $\langle r \rangle$, was calculated by using the equation

$$\langle r \rangle = \frac{I_{VV} - G I_{VH}}{I_{VV} + 2G I_{VH}} \qquad (3)$$

where the subscript pairs, H and V, give the orientations (horizontal and vertical) of the excitation and emission polarizers, respectively, and $G = I_{HV}/I_{HH}$ is an instrument correction factor.

The dependence of the steady-state fluorescence anisotropy, $\langle r \rangle$, on protein concentration for a dimer−tetramer equilibrium is given by the equation

$$\langle r \rangle = (\langle r \rangle_d((K_d^2 + 4K_d[P_t])^{1/2} - K_d) + \langle r \rangle_t(2[P_t] + K_d - (K_d^2 + 4K_d[P_t])^{1/2}))/2[P_t] \qquad (4)$$

in which $[P_t]$ is the total protein concentration (subunits), $\langle r \rangle_d$ is anisotropy for the dimer, $\langle r \rangle_t$ is anisotropy for the tetramer, and K_d is the apparent dissociation constant for the dimer−tetramer equilibrium. For the fitting of data to eq 4, Kaleidagraph was used, and the values for $\langle r \rangle_d$ and $\langle r \rangle_t$ were fixed at 0.241 and 0.222, respectively. The value for $\langle r \rangle_d$ was obtained from the fit of the data at 0 mM FBP, and the value for $\langle r \rangle_t$ was obtained by fitting the remaining data with $\langle r \rangle_d$ fixed at 0.241. These values provide the smallest χ^2 in the fits.

The linkage between FBP binding and the dimer−tetramer equilibrium is treated according to the theory of linked functions in ligand binding (*28*). Two linkage functions can be defined for this system. The first function expresses the dependence of the fractional saturation of FBP binding on protein concentration. The second function expresses the dependence of the apparent K_d for the dimer−tetramer equilibrium on the concentration of FBP and is the function that is directly applicable to studies described here. This linkage function is obtained by multiplying the dissociation constant in the absence of FBP by the ratio of the FBP-binding polynomials for the dimer and tetramer and is given by eq 5 (*28*). The equilibrium constants in eq 5, which are

Scheme 1: Linkage between FBP Binding and the Dimer−Tetramer Equilibrium

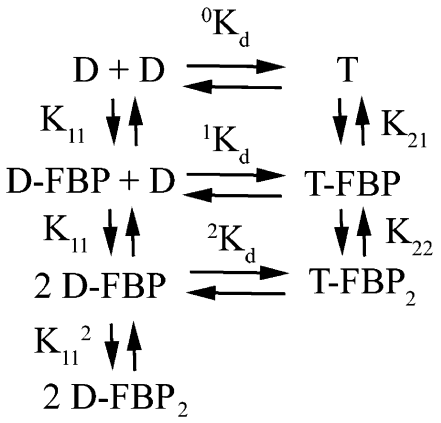

$$K_d^{app} = \frac{{}^0K_d((1 + [\text{FBP}]/K_{11})^2)^n}{1 + 2[\text{FBP}]/K_{21} + [\text{FBP}]^2/K_{21}K_{22}} \qquad (5)$$

obtained by fitting the data by using Kaleidagraph, are dissociation constants for the reactions that are shown in Scheme 1, in which D represents the dimer; T represents the tetramer; ^0K_d is the dimer−tetramer dissociation constant in the absence of FBP; K_{11} is the intrinsic dissociation constant for FBP binding to unliganded (with respect to FBP) or singly liganded dimer; K_{21} and K_{22} are intrinsic dissociation constants for FBP binding to unliganded (with respect to FBP) and singly liganded tetramer, respectively; and n is the stoichiometry for FBP binding to a dimer. Noncooperative binding of FBP to the dimer is assumed. The stoichiometry for FBP binding to the tetramer is two sites per tetramer, which is based on the crystal structure of the complex (*13*).

Three cases can be considered for the dimer FBP-binding stoichiometry, n, in systems of the type exemplified by these kinase and dehydrogenase families, and each case predicts a different dependence of the apparent K_d on FBP concentration. For $n = 0$, FBP does not display measurable affinity for binding to the half-sites of the dimer. In this case, the dimer binding polynomial in the numerator of eq 5 is equal to 1, and the apparent K_d decreases monotonically without bound as the concentration of FBP increases. For $n = 1$, the stoichiometry for FBP binding to the dimer and tetramer is the same, which is consistent with dissociation of the tetramer along the interface which does not contain the FBP-binding sites, i.e., interface 1 in Figure 1. In this case, the apparent K_d decreases as the concentration of FBP increases, but its value reaches a plateau which is the value of the dissociation constant in the saturating presence of FBP. For $n = 2$, the stoichiometry for FBP binding increases from two complete sites per tetramer to four half-sites per pair of dimers, which

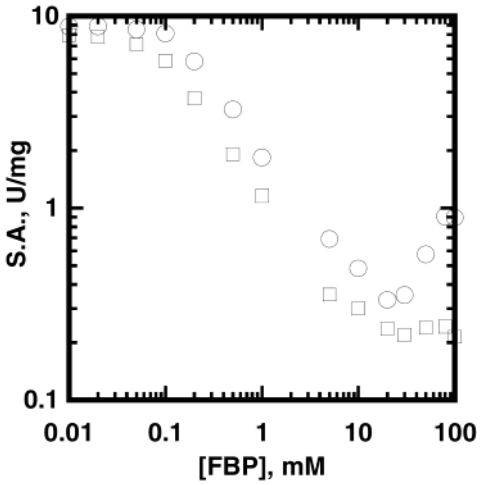

FIGURE 3: Critical behavior in the FBP concentration dependence of inhibition of catalysis. The FBP concentration dependence of the specific activity (SA) of E478C glycerol kinase was determined at 2 mM glycerol and 0.2 mM ATP. Conditions: pH 7.0, 25 °C. Legend: enzyme concentration (nM subunits); ○, 5.4; □, 54.

is consistent with dissociation of the tetramer along the interface which contains the FBP-binding sites, i.e., interface 2 in Figure 1. In this case, the apparent K_d shows critical behavior as the concentration of FBP increases: the apparent K_d decreases and then increases, displaying a minimum. The occurrence of critical behavior in such systems has been considered in theory (*25*, *29*) and characterized experimentally for binding of ATP to human methemoglobin A (*25*).

RESULTS AND DISCUSSION

FBP Inhibition Displays Critical Behavior Arising from Increased Ligand Stoichiometry upon Tetramer Dissociation. To evaluate whether FBP may show measurable affinity for binding to the half-sites in the dimer, we determined the FBP concentration dependence of allosteric inhibition at two different protein concentrations. Results of this experiment are shown in Figure 3.

At both protein concentrations, inhibition by FBP is observed as the concentration of FBP in the assay is increased from zero. At the lower protein concentration, a minimum of specific activity is seen at about 20 mM FBP, with the specific activity increasing as the concentration of FBP is increased above this value. That is, the FBP concentration dependence of the specific activity displays critical behavior. At the higher protein concentration, the specific activity appears to reach a plateau at the higher concentrations of FBP, and critical behavior is not observed. The dependence of the critical behavior on protein concentration shows that it does not reflect artifacts or changes in ionic strength that occur at the high FBP concentrations that are used in these determinations. At the higher protein concentration, the apparent $K_{0.5}$ is decreased, and the specific activity reaches a lower value. Both of these results are consistent with the expected increase in the fraction of tetramer. The dependence of FBP inhibition on protein concentration is consistent with the dimer−tetramer equilibrium, where the lower concentrations of FBP shift the equilibrium toward the tetramer. The critical behavior that is observed at the lower protein concentration is consistent with decreased inhibition at higher FBP concentrations due to dimer dissociation that arises from the increased stoichiometry for FBP. Importantly, these results show that FBP has measurable affinity for binding to the half-sites on the dimer. The decreased inhibition indicates that binding of FBP to the dimer does not inhibit the catalytic activity to the same extent as it does for the tetramer.

A linkage analysis of the specific activity results that are shown in Figure 3, which would define the coupling between FBP binding and oligomeric state, is complex. It requires knowledge of the dimer−tetramer dissociation constant, FBP affinities for the dimer and tetramer, the specific activities of all the enzyme forms that are present in the assay, and the relations between binding of FBP and substrates. An important aspect of such studies would be determination of the protein concentration dependencies of the catalytic properties. However, variation of the protein concentration over the necessary range is not feasible with the continuous coupled spectrophotometric assay. There is, however, an experimental approach that will yield the affinities for FBP binding to the dimer and tetramer and the dissociation constants for the dimer−tetramer equilibrium: analysis of the linkage between FBP binding and the dimer−tetramer dissociation reaction in the absence of catalysis.

The equilibrium relations that obtain for this linkage are shown in Scheme 1, where D represents the dimer; T represents the tetramer; ${}^0K_d$ is the dimer−tetramer dissociation constant in the absence of FBP; K_{11} is the intrinsic dissociation constant for FBP binding to dimer; K_{21} and K_{22} are intrinsic dissociation constants for FBP binding to unliganded (with respect to FBP) and singly liganded tetramer, respectively, and the remaining equilibrium constants are the dissociation constants for the reactions that are indicated.

Evaluating the linkage to obtain estimates of the dissociation constants that define it requires determination of the FBP concentration dependence of the oligomeric state of the enzyme. Because the methods that were used in earlier studies either are not sufficiently sensitive to observe the dimer−tetramer equilibrium or yield highly disparate values for its dissociation constant, we use a new approach for studies of the coupling between FBP binding and the dimer−tetramer equilibrium.

Labeling an Engineered Surface Cysteine Residue with Extrinsic Fluorophores. We constructed the E478C variant of glycerol kinase in earlier studies of the cation-promoted association by Zn(II) of binding of IIA^{Glc}, which is a second allosteric inhibitor (*26*). The engineered cysteine residue is located on the surface of the glycerol kinase subunit, as shown in Figure 1. The sites of the substitutions are about 50 Å apart in both the dimer and the tetramer. The E478C site is about 30 Å from the active site and about 70 Å from the FBP-binding site. The distances between the E478C sites in the dimer and tetramer are near the Förster distances for several extrinsic fluorophores (*30*), suggesting that fluorescence energy transfer methods might be used to characterize quantitatively the coupling between the dimer−tetramer equilibrium and binding of FBP. Because of the symmetrical distances between the E478 positions, the observation of energy transfer is not dependent on the tetramer interface at which dissociation occurs. For the small protein melittin, fluorescence depolarization due to homo-FRET between fluorescein moieties covalently attached as extrinsic fluoro-

Table 1: Effects of Labeling E478C Glycerol Kinase with 0.36 mol of OG/mol of Subunit on Initial Velocity and FBP Inhibition Parameters[a]

glycerol kinase	V_{max} (units/mg)	K_{ATP} (μM)	K_{gol} (μM)	K_{iATP} (μM)	I_{max} (%)	n_H	$K_{0.5}$ (mM)
native	14.3 ± 0.6	9 ± 2	5 ± 2	86 ± 43	94 ± 2	1.5 ± 0.1	0.33 ± 0.02
E478C	4.8 ± 0.1	7 ± 1	3 ± 1	46 ± 11	95 ± 2	1.4 ± 0.2	0.18 ± 0.02
E478C-OG	4.6 ± 0.1	10 ± 1	4 ± 1	36 ± 8	94 ± 2	1.5 ± 0.2	0.19 ± 0.02

[a] Steady-state kinetic parameters were obtained from fits of initial velocity data to eq 1, and FBP inhibition parameters were obtained from fits of initial velocity data to eq 2. Conditions: 0.1 M TEA, pH 7.0, 25 °C.

phores was used to characterize oligomerization (*31*). We show below that this approach can be used to characterize the linkage between FBP binding and oligomerization of glycerol kinase.

Glycerol kinase contains five native cysteine residues per subunit at sequence positions 105, 112, 255, 269, and 292 (*27*). We reported the effects of treatment of glycerol kinase with sulfhydryl reagents (*32*). Incubation of native glycerol kinase at pH 7.0 and 25 °C with millimolar concentrations of the sulfhydryl group-specific reagent *N*-ethylmaleimide or 5,5′-dithiobis(2-nitrobenzoic acid) results in loss of catalytic activity, and the rate of inactivation is decreased greatly by addition of glycerol or ATP. Incubation with 0.1 M iodoacetate for 30 min does not cause inactivation. We evaluated whether the native cysteine residues could be protected from labeling with the extrinsic fluorophores by adding active site ligands to the labeling reaction and by choosing iodoacetamido derivatives of the fluorophores. In preliminary experiments, we incubated native and E478C glycerol kinases (2 μM subunits) with iodoacetamidofluorescein (5-fold molar excess) for 1 h at pH 7.0 or 8.0 at ambient temperature in the absence and presence of 2 mM glycerol plus 2 mM ATP. The reactions were quenched with 1 mM β-mercaptoethanol, and the proteins were loaded onto SDS−PAGE gels. After electrophoresis, UV light was used to determine visually whether labeling of the proteins occurred. The substrates prevent labeling of the native enzyme but not the E478C variant.

The progress curve for reaction of E478C glycerol kinase with iodoacetamido-OG at pH 8 and ambient temperature was constructed by determining the labeling stoichiometry as a function of incubation time. Aliquots were removed during the time course and quenched with β-mercaptoethanol. Unincorporated fluorescent label was removed by gel permeation chromatography and dialysis. At an enzyme concentration of 0.5 mg/mL [9 μM (subunits)] and a 5-fold molar excess of iodoacetamido-OG, the enzyme is labeled to 0.1 mol of OG/mol of subunit in about 3 min. The rate of labeling decreases thereafter, likely due to competing hydrolysis of the iodoacetamido moiety. The labeling stoichiometry reaches about 0.20 mol of OG/mol of subunit at 10 min and a plateau of about 0.35 mol of OG/mol of subunit by 60 min of incubation. The native glycerol kinase is not labeled detectably under these conditions. The time course of labeling of the E478C variant glycerol kinase and the absence of detectable labeling of the native enzyme suggest that the engineered surface cysteine residue is specifically labeled under these conditions. Peptide mapping and MALDI-MS were utilized to test this hypothesis.

Native or E478C variant glycerol kinase was incubated separately with the iodoacetamido derivative of fluorescein or OG at pH 8.0 for 1 h at ambient temperature as described for the progress curve. This treatment labeled the E478C variant with 0.38 mol of fluorescein or 0.35 mol of OG/mol of subunit. No incorporation into the native glycerol kinase was observed ($\ll$0.01 mol of fluorophore/mol of subunit). The specific activity of the E478C enzyme is not altered by the labeling reaction. The enzymes were digested with trypsin, and the peptides were separated by using HPLC with the absorbance monitored at 490 and 215 nm. No peaks with absorbance at 490 nm are observed for native glycerol kinase. The fluorescein-labeled E478C enzyme shows a single peak of absorbance at 490 nm, and the OG-labeled E478C enzyme shows two peaks. Each A_{490} peak and the neighboring A_{215} peaks were collected manually and analyzed by MALDI-MS. Each of the A_{490} peaks contains a species with the molecular mass that corresponds to the peptide of the E478C variant glycerol kinase residues 469−479 with a covalently attached fluorophore (fluorescein, 1696 Da; OG, 1732 Da). This species is consistent with the peptide that represents cleavage by trypsin at R468 and R479 and thus contains the E478C substitution. This peptide also contains R471, which is not a tryptic cleavage site because its C-terminal peptide bond partner is P472. A likely explanation for the two peaks which contain the same labeled peptide that are observed for the OG-labeled glycerol kinase is the presence of 5- and 6-isomers in the commercial preparation of iodoacetamido-OG (Molecular Probes, Inc., catalog) and differences in the HPLC elution of the peptide with each isomer.

The OG-labeled E478C glycerol kinase was used for the studies that are reported below. The studies conducted here are performed at pH 7.0, and the pK_a for ionization of fluorescein and OG is 6.4 and 4.8, respectively (Molecular Probes, Inc.). Use of the OG-labeled enzyme thus obviates questions about the sensitivity of the observed fluorescence properties to changes in ionization of the probe. However, the same results are obtained for E478C glycerol kinase labeled with either intrinsic fluorophore.

These peptide chemistry results indicate that the extrinsic fluorophores label specifically the engineered surface cysteine residue, and no labeling of the native cysteine residues is detected when these labeling conditions are used. Incubations at higher initial label:enzyme ratios result in labeling of native cysteine residues, as shown by decreased specific activity, more extensive labeling, and the appearance of other peaks of A_{490} absorbance in the HPLC elution profiles.

Effects of the Conjugated Fluorophore on the Catalytic and FBP Regulatory Properties. Labeling of the E478C variant glycerol kinase to a stoichiometry of 0.36 mol of OG/mol of subunit does not alter the catalytic or FBP regulatory properties of the enzyme. This is shown in Table 1, where initial velocity and FBP inhibition parameters for the native, E478C, and E478C-OG glycerol kinases are summarized.

Table 2: Effects of Protein Concentration and Ligands on Fluorescence Anisotropy of E478C Glycerol Kinase Labeled with ~0.1 mol of OG/mol of Subunit[a]

[glycerol kinase] [nM (subunits)]	[FBP] (mM)	steady-state anisotropy			
		no addition	2 mM gol	2 mM ATP	2 mM gol/ 2 mM ATP
36	0	0.268 ± 0.009	−0.015 ± 0.003	−0.003 ± 0.002	−0.014 ± 0.002
	5	−0.003 ± 0.002	−0.014 ± 0.003	−0.004 ± 0.002	−0.016 ± 0.003
360	0	0.266 ± 0.008	−0.014 ± 0.002	−0.004 ± 0.002	−0.013 ± 0.002
	5	−0.002 ± 0.002	−0.014 ± 0.003	−0.004 ± 0.003	−0.015 ± 0.003

[a] The absolute value of the anisotropy (mean ± standard deviation) obtained in the absence of ligands for three independent labeling experiments is shown in the row "0 mM FBP" and column "no addition" for each enzyme concentration. The remaining values are shown as the change in anisotropy (mean ± standard deviation) upon addition of the indicated concentration of ligand, where the change is given by the relation $\Delta\langle r\rangle = \langle r\rangle_{+\text{ligand}} - \langle r\rangle_{-\text{ligand}}$, and $\langle r\rangle$ is the observed steady-state anisotropy. Conditions: 0.1 M TEA, pH 7.0, 25 °C.

The E478C substitution itself decreases V_{max} and decreases the $K_{0.5}$ for FBP inhibition relative to the native enzyme, as shown previously (*26*). Labeling of the variant glycerol kinase with OG does not change further any of the catalytic or FBP regulatory parameters. The same results are obtained for enzyme labeled with fluorescein (not shown). Thus, the extrinsic fluorophore provides a reporter group that does not measurably perturb the functional properties of interest.

Depolarization of Fluorescence Anisotropy by Homo-FRET Is Dependent on Labeling Stoichiometry. The fluorescence anisotropy of the conjugated extrinsic fluorophore is expected to be affected by its molecular motions, its lifetime, and homo-FRET. Contributions to the anisotropy due to global rotation of the protein should be obviated by the large size of glycerol kinase (56 kDa/subunit) and its concomitant slow rotational motion [calculated rotational correlation time >70 ns for the dimer (*30*)] relative to the lifetimes of these fluorophores (~4 ns). The occurrence of homo-FRET is dependent on the labeling stoichiometry. If the reactivity of each site is identical and independent of the extent of labeling, the fraction of tetramers with 0, 1, 2, 3, or 4 labels is 0.66, 0.29, 0.05, 0, and 0, respectively, for a labeling stoichiometry of 0.1 mol of fluorophore/mol of subunit. For this low labeling stoichiometry, effects due to homo-FRET should be eliminated because of the very small populations of multiply labeled species. Thus, at the low labeling stoichiometries, only local molecular motions and changes in lifetime are expected to alter the anisotropy. At a labeling stoichiometry of 0.40 mol of fluorophore/mol of subunit, the fraction of tetramers containing 0, 1, 2, 3, or 4 fluorophores is 0.13, 0.35, 0.35, 0.15, and 0.03, respectively. Because of the increased populations of multiply labeled species at the higher stoichiometry, depolarization due to homo-FRET is expected to alter the anisotropy.

The dependence of the steady-state anisotropy on labeling stoichiometry shows that the anisotropy conforms to these expectations. The E478C variant glycerol kinase was labeled with OG to stoichiometries of 0.01−0.36 mol of OG/mol of subunit by quenching the labeling reaction with β-mercaptoethanol after increasing times of incubation. After dialysis, the labeling stoichiometry was determined from absorbance measurements, the samples were adjusted to 90 nM (subunits), and the fluorescence anisotropy in the absence of added ligands was determined. A single value, 0.256 ± 0.002 ($n = 5$), is observed for the anisotropy for enzyme that is labeled to stoichiometries of 0.01−0.11 mol of OG/mol of subunit. For labeling stoichiometries of 0.12−0.36 mol of OG/mol of subunit, the anisotropy decreases in a linear fashion to a value of 0.232 at the highest stoichiometry. These results are consistent with the expected absence of homo-FRET for stoichiometries less than ~0.1 mol of OG/mol of subunit due to undetectably small populations of multiply labeled enzyme species and with decreased anisotropy at higher labeling stoichiometries because of depolarization due to homo-FRET, which reflects increasing populations of multiply labeled species. The anisotropy observed at the lower labeling stoichiometries is less than that expected for completely immobilized OG (~0.34), indicating that the probe undergoes local motions and/or its lifetime is increased relative to unconjugated OG. The emissivity of the conjugated OG is much less than that of unconjugated OG, so increased lifetime is unlikely to account for the lower anisotropy.

The sensitivity of anisotropy in the absence of homo-FRET to protein concentration and ligand binding was evaluated by using E478C glycerol kinase that was labeled to ~0.1 mol of OG/mol of subunit. Because this labeling stoichiometry obviates homo-FRET and the long global rotational correlation time obviates effects of global rotation, only local molecular motions and changes in lifetime are expected to alter the anisotropy. Results of these studies are presented in Table 2.

In the absence of added ligands, the difference between absolute values of observed anisotropy for the protein concentrations of 36 and 360 nM (subunits) is 0.002 ± 0.012 ($n = 3$). The results that were obtained for the absolute anisotropy show higher uncertainty than expected (0.008−0.009 versus 0.002−0.003). This greater degree of uncertainty appears to reflect instrument variations over the several days time between individual experiments. Within the precision of the data, the anisotropy does not depend on protein concentration. Results that are described below support this conclusion.

The effects of ligand addition on the anisotropy are shown as the change in anisotropy relative to the value obtained at the respective protein concentration in the absence of ligands. The changes in anisotropy obtained for experiments performed on the same day for the different ligands show the expected range of uncertainty (0.002−0.003). This result shows that the apparent instrument variation does not occur over the course of an individual experiment, and the small uncertainties in the anisotropy changes show that the ligand effects are highly reproducible despite the variability of the absolute anisotropies. Addition of glycerol decreases the anisotropy substantially. Addition of ATP may decrease the anisotropy by a very small amount. The combination of

glycerol plus ATP gives the same decrease as seen for glycerol alone. The anisotropy is not changed significantly at either protein concentration by addition of FBP, and FBP does not change the effects of glycerol or ATP on the anisotropy.

Because of the absence of homo-FRET and contributions of global rotation, the decreased anisotropy observed for glycerol indicates increased local motions and/or lifetime of the fluorophore. The distance between the active site and the E478C substitution site is ~30 Å, so effects of glycerol must be mediated via a conformational change. Glycerol binding is believed to promote an active site closure similar to that observed for glucose binding to the related superfamily member hexokinase (*18*, *33*), and such a conformational change is the likely explanation for the decrease in anisotropy due to glycerol binding. Binding of ATP alone is associated with a conformational change, as shown by its protection of the native cysteine residues from modification by sulfhydryl reagents (*32*). However, the conformational change is different from that seen for glycerol because ATP has little, if any, effect on the anisotropy. Since FBP is known to promote tetramer assembly, the lack of effect of FBP on the anisotropy in the absence or presence of other ligands shows that the population of multiply labeled tetramers is below experimentally detectable levels, as expected at this lower labeling stoichiometry. The absence of an observable effect of FBP on the anisotropy suggests that any conformational changes associated with FBP binding, including dimer association to form tetramers, do not alter the local mobility and/or lifetime of the conjugated fluorophore. Although offsetting and compensating effects on mobility and lifetime are possible, it seems unlikely that such effects would be compensatory for both glycerol and ATP.

The results obtained at these lower stoichiometries of labeling indicate that the fluorescence anisotropy of OG that is conjugated to the engineered surface cysteine residue of the E478C glycerol kinase variant displays the behavior that is expected in the absence of homo-FRET. It is altered by changes in local mobility and/or lifetime but is not sensitive to changes in the oligomeric structure of the enzyme or binding of FBP.

Decreased Fluorescence Anisotropy Due to Homo-FRET Is Described by a Dimer−Tetramer Equilibrium. To determine the effects of homo-FRET on the anisotropy of the conjugated fluorophore, the E478C variant glycerol kinase was labeled to a stoichiometry of 0.38 mol of OG/mol of subunit. Because of the greater fraction of multiply labeled tetramers at this label stoichiometry, changes in the extent of tetramer formation are expected to alter the fluorescence anisotropy because of depolarization due to homo-FRET. Figure 4 shows that this is the case. It shows the dependence of the anisotropy on protein concentration at different concentrations of FBP in the saturating presence of glycerol. At 0 mM FBP, a significant decrease in anisotropy occurs as the protein concentration is increased over the range 2−900 nM (subunits). A significant decrease is seen also by comparing the anisotropies at the two protein concentrations that were used for the experiments in Table 2, 36 and 360 nM. This result is consistent with homo-FRET that is expected upon association of labeled dimers to produce multiply labeled tetramers. It supports the conclusion reached for the lower labeling stoichiometry that the lack of sensitivity of the anisotropy to protein concentration reflects small populations of multiply labeled tetramers rather than the absence of tetramer formation. In the absence of glycerol, no change in anisotropy is observed over this range of protein concentration. This result indicates that tetramer formation is coupled to the binding of glycerol.

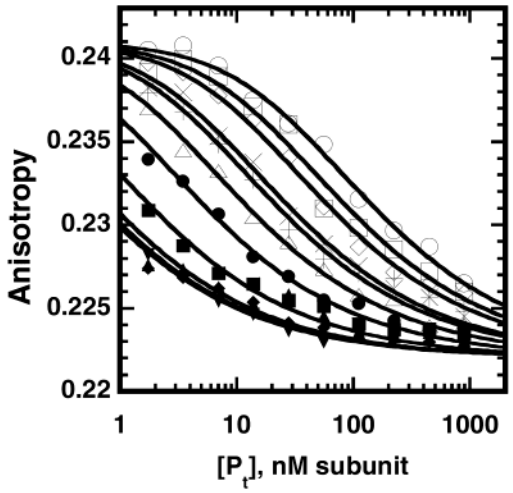

FIGURE 4: Dependence of the fluorescence anisotropy of OG-labeled E478C glycerol kinase on protein and FBP concentrations. E478C glycerol kinase was labeled to 0.38 mol of OG/mol of subunit. Fluorescence anisotropy was determined at the protein concentrations shown in the figure and the following concentrations of FBP (mM): ○, 0; □, 0.05; ◇, 0.1; ×, 0.2; +, 0.3; △, 0.5; ●, 1; ■, 5; ◆, 10; ▲, 20; ▼, 50. The points show the data, and the lines show the best fit to eq 4 with $\langle r\rangle_d = 0.241$ and $\langle r\rangle_t = 0.222$. Conditions: 0.1 M TEA, 2 mM glycerol, 0.1 mM EDTA, 0.1 mM β-mercaptoethanol, pH 7.0, and 25 °C.

The protein concentration dependence of the anisotropy at 0 mM FBP is well described by eq 4, as shown by the fitted line in Figure 4. Equation 4 describes the association reaction in terms of an equilibrium between dimers and tetramers, and the fit yields an apparent dissociation constant of 61 ± 7 nM (subunits) at pH 7.0 and 25 °C. The data are well described by the equation, indicating that a dimer−tetramer equilibrium is consistent with the protein concentration dependence of the anisotropy. The fitted dissociation constant is in good agreement with the values of 25−57 nM (subunits) obtained at the same experimental conditions from estimating the rate constants for the component association and dissociation reactions and from small-zone analytical gel permeation chromatography (*21*, *22*).

Coupling between FBP Binding and the Dimer−Tetramer Equilibrium. Figure 4 shows the protein concentration dependency of the anisotropy change for enzyme that is labeled with OG to higher stoichiometry is sensitive to addition of FBP. Examination of the results obtained for protein concentrations that are the same as those in Table 2, 36 and 360 nM, shows that addition of FBP decreases the anisotropy substantially. This result contrasts that obtained at the lower labeling stoichiometry where no change is seen. The decreased anisotropy is consistent with FBP-dependent tetramer formation and concomitant depolarization because of homo-FRET due to the larger populations of multiply labeled tetramers.

Addition of FBP shifts the protein concentration dependence of the anisotropy change to lower concentrations. The dependence of the anisotropy on protein concentration at each

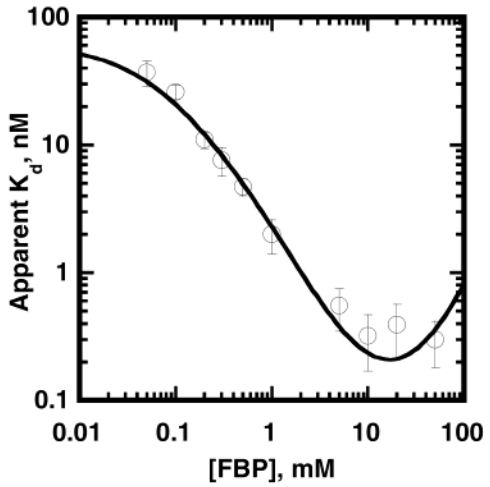

FIGURE 5: Dependence of the apparent K_d for the dimer−tetramer equilibrium on FBP concentration. The points show the values of the apparent K_d with their standard errors as obtained from the fits of the data in Figure 4. The line shows the best fit, weighted by the standard error, to eq 5 with $n = 2$, yielding parameters that are given in the text.

concentration of FBP was fitted to eq 4 to obtain an apparent K_d for the dimer−tetramer dissociation reaction. The lines in Figure 4 show that the anisotropy data at each FBP concentration are well described by eq 4, indicating that FBP does not change the mode of association. The values of apparent K_d that are obtained from the fits are plotted as a function of the concentration of FBP in Figure 5. As shown by the fitted line in Figure 5, the FBP concentration dependence of the apparent K_d is well described by eq 5 with $n = 2$. The fit yields the following values for parameters shown in Scheme 1: ${}^0K_d$, 64 ± 8 nM; K_{11}, 19 ± 5 mM; K_{21}, 0.10 ± 0.02 mM; K_{22}, 0.79 ± 0.63 mM; ${}^2K_d$, 0.014 ± 0.013 nM.

The fitted value for ${}^0K_d$ agrees well with the value obtained from the fit to the data with 0 mM FBP, indicating that the data are self-consistent. The dissociation constant ${}^2K_d$ was calculated from the relation, ${}^2K_d = {}^0K_dK_{21}K_{22}/(K_{11})^2$, and its uncertainty is that obtained by standard propagation of the errors in the other dissociation constants. For each of the fitted parameters except K_{22}, the value of the uncertainty shows that the dissociation constants are well determined by the data. The relatively large uncertainty in the value of K_{22} contributes to the large uncertainty in the calculated value for ${}^2K_d$. Despite the large uncertainty in the fitted value for K_{22}, it is different from the value for K_{21}. If the values for K_{21} and K_{22} are constrained to be the same in the fitting, a much poorer fit of the data is obtained. Overall, the coupling between FBP binding and the dimer−tetramer reaction is quite well defined by eq 5 with $n = 2$ and reveals important information about FBP binding in the saturating presence of glycerol.

The coupling between FBP binding and tetramer formation is given by the ratio ${}^0K_d/{}^2K_d$, which is 4570 ± 4200. The coupling free energy that this ratio gives is −5.0 (−3.5, −5.4) kcal/mol. It is similar in magnitude, although opposite in sign, to the value of about 6 kcal/mol (heme) for the coupling between oxygen binding and the dimer−tetramer equilibrium for human hemoglobin (*34*). Because of linkage relationships, the same ratio applies to the relative FBP-binding affinities of the dimer and tetramer; i.e., the affinity is about 4000-fold greater for FBP binding to the tetramer than to the dimer.

FBP inhibition of catalysis displays positive cooperativity as shown by the values of the Hill coefficients in Table 1, which are greater than 1. One possible source of the positive cooperativity is positive coupling between the FBP-binding sites of the tetramer. However, the fitted values for K_{21} and K_{22} show that FBP binding to the tetramer displays weak negative coupling. The positive cooperativity of inhibition is thus not due to positive coupling between the FBP sites. A second possible source of the positive cooperativity is the 4000-fold difference between the affinity for FBP binding to the tetramer versus the dimer. The value of ${}^0K_d$ indicates that, at the protein concentrations typically used for the inhibition determinations [10 nM (subunits)], a substantial population of dimer is present. Results of these studies strongly suggest that the difference in FBP affinity of the dimer versus tetramer is the basis for the positive cooperativity of FBP inhibition. One difference between these binding experiments and the inhibition experiments is the presence of the second substrate MgATP in the inhibition experiments. Although saturating concentrations of glycerol are present in these binding experiments, the role of MgATP is not considered in Scheme 1 and may influence the coupling in the case of FBP inhibition.

The data in Figure 5 show clearly that binding of FBP to the dimer of glycerol kinase must be explicitly considered in any model that describes FBP binding. If FBP does not bind to the dimer, the apparent K_d decreases without bound as FBP is increased, and this is not seen in the figure. Both structural and functional evidence shows that treatment of FBP binding to the dimer must explicitly consider the increased stoichiometry that occurs upon tetramer dissociation. The novel symmetric, bimodal binding of FBP to the tetramer (*13*) provides a basis for two half-sites generated from a single site in the tetramer if the tetramer dissociates along the same interface that contains the FBP-binding sites. Results of site-directed mutagenesis studies of glycerol kinases (*17*, *18*) and the L-lactate dehydrogenases (*19*) show that tetramer dissociation occurs along the interface with the FBP-binding sites. The observation of critical behavior in both FBP inhibition and the linkage between FBP binding and the dimer−tetramer dissociation reaction shows that FBP binds to sites other than those seen in the crystal structure of the tetramer−FBP complex. There is no evidence for other sites for FBP binding in this complex despite the presence of 25 mM FBP in the crystals (*13*). Although other sites could be masked by crystal contacts, the most likely explanation for the other sites is the increased stoichiometry that occurs upon tetramer dissociation to generate from two complete sites four half-sites with greatly reduced affinity for FBP. This explanation is consistent with the loss of critical behavior when the protein concentration is increased.

The increased ligand stoichiometry for FBP that occurs upon tetramer dissociation must be accounted for in the analysis of the linkage between FBP binding and the dimer−tetramer equilibrium. If the increased stoichiometry is ignored, eq 5 with $n = 1$ provides a good fit of the FBP concentration dependence of the apparent K_d for the dimer−tetramer dissociation reaction. However, the value for K_{11} is about 10-fold smaller, indicating a greater affinity for FBP binding to the dimer and smaller coupling between FBP binding and tetramer formation. The coupling free energy

is underestimated by about 1.8 kcal/mol. Failure to account for the increased FBP stoichiometry thus results in an erroneous assessment of the linkage between FBP binding and the dimer−tetramer dissociation.

For the case of human hemoglobins, characterization of the coupling between oxygen binding and dimer−tetramer assembly has provided important insights into the molecular basis for allosteric regulatory behavior (*24*). In such studies, change in oligomeric state is viewed not as an experimental complication but as an important tool for accessing protein molecular behavior and properties. Indeed, for these types of regulatory systems, a linkage study approach is essential for obtaining the equilibrium constants that describe ligand binding to the different oligomeric states. Evaluation of the coupling between FBP binding and the dimer−tetramer equilibrium of *E. coli* glycerol kinase shows that the affinity for FBP binding to the tetramer is about 4000-fold greater than for binding to the dimer. Yet, because of the increased FBP stoichiometry that occurs upon tetramer dissociation due to the mode of FBP binding, sufficiently high concentrations of FBP shift the equilibrium toward the dimer. An important practical consequence of this novel behavior is that the relative affinities for ligand binding to the dimer and tetramer can only be determined by using the approach of linked functions as described here. Isolation of one form or the other by manipulating concentrations of protein and/or ligand to enable characterization of its binding properties is not feasible because of the coupled binding and increased ligand stoichiometry upon dissociation.

The increased FBP stoichiometry of the dimer relative to the tetramer could have a role in vivo by ensuring that the FBP inhibition occurs only if the concentration of glycerol kinase is sufficiently high. Because of the similarity in the apparent modes of FBP binding for glycerol kinases and the bacterial L-lactate dehydrogenases, the apparent dissociation constant for tetramer assembly and the FBP activation of the dehydrogenases may show also critical behavior with respect to FBP concentration dependence under appropriate experimental conditions.

ACKNOWLEDGMENT

We thank Dr. Larry Dangott of the Protein Chemistry Laboratory of Texas A&M University for the peptide mapping and MALDI-MS and Dr. Gregory D. Reinhart for helpful discussions. We are grateful for helpful comments from one of the reviewers.

REFERENCES

1. Allen, S. J., and Holbrook, J. J. (2000) *Protein Eng. 13*, 5−7.
2. Arai, K., Hishida, A., Ishiyama, M., Kamata, T., Uchikoba, H., Fushinobu, S., Matsuzawa, H., and Taguchi, H. (2002) *Protein Eng. 15*, 35−41.
3. Iwata, S., and Ohta, T. (1993) *J. Mol. Biol. 230*, 21−27.
4. Kotik, M., and Zuber, H. (1993) *Eur. J. Biochem. 211*, 267−280.
5. Yamada, T., and Carlsson, J. (1975) *J. Bacteriol. 124*, 55−61.
6. Lin, E. C. C. (1996) in *Escherichia coli and Salmonella. Cellular and molecular biology* (Neidhardt, F. C., Ed.) pp 307−342, ASM Press, Washington, DC.
7. Pawlyk, A. C., and Pettigrew, D. W. (2001) *Protein Expression Purif. 22*, 52−59.
8. Berman, M., and Lin, E. C. C. (1971) *J. Bacteriol. 103*, 113−120.
9. Zwaig, N., and Lin, E. C. C. (1966) *Science 153*, 755−757.
10. Zwaig, N., Kistler, W. S., and Lin, E. C. C. (1970) *J. Bacteriol. 102*, 753−759.
11. Pettigrew, D. W., Liu, W. Z., Holmes, C., Meadow, N. D., and Roseman, S. (1996) *J. Bacteriol. 178*, 2846−2852.
12. Holtman, C. K., Pawlyk, A. C., Meadow, N. D., and Pettigrew, D. W. (2001) *J. Bacteriol. 183*, 3336−3344.
13. Ormö, M., Bystrom, C. E., and Remington, S. J. (1998) *Biochemistry 37*, 16565−16572.
14. Wigley, D. B., Gamblin, S. J., Turkenburg, J. P., Dodson, E. J., Piontek, K., Muirhead, H., and Holbrook, J. J. (1992) *J. Mol. Biol. 223*, 317−335.
15. Christopher, J. A. (1996) SPOCK, Center for Macromolecular Design, Texas A&M University, College Station, TX.
16. Guex, N., and Peitsch, M. C. (1997) *Electrophoresis 18*, 2714−2723.
17. Liu, W. Z., Faber, R., Feese, M., Remington, S. J., and Pettigrew, D. W. (1994) *Biochemistry 33*, 10120−10126.
18. Bystrom, C. E., Pettigrew, D. W., Branchaud, B. P., O'Brien, P., and Remington, S. J. (1999) *Biochemistry 38*, 3508−3518.
19. Jackson, R. M., Gelpi, J. L., Cortes, A., Emery, D. C., Wilks, H. M., Moretono, K. M., Halsall, D. J., Sleigh, R. N., Behan-Martin, M., Jones, G. R., Clarke, A. R., and Holbrook, J. J. (1992) *Biochemistry 31*, 8307−8314.
20. Thorner, J. W., and Paulus, H. (1971) *J. Biol. Chem. 246*, 3885−3894.
21. de Riel, J. K., and Paulus, H. (1978) *Biochemistry 17*, 5141−5146.
22. de Riel, J. K., and Paulus, H. (1978) *Biochemistry 17*, 5134−5140.
23. Feese, M. D., Faber, H. R., Bystrom, C. E., Pettigrew, D. W., and Remington, S. J. (1998) *Structure 6*, 1407−1418.
24. Ackers, G. K. (1998) *Adv. Protein Chem. 51*, 185−253.
25. Baghurst, P. S., and Nichol, L. W. (1975) *Biochim. Biophys. Acta 412*, 168−180.
26. Pettigrew, D. W., Meadow, N. D., Roseman, S., and Remington, S. J. (1998) *Biochemistry 37*, 4875−4883.
27. Pettigrew, D. W., Ma, D.-P., Conrad, C. A., and Johnson, J. R. (1988) *J. Biol. Chem. 263*, 135−139.
28. Wyman, J. C., and Gill, S. J. (1990) *Binding and Linkage: Functional Chemistry of Biological Macromolecules*, University Science Books, Mill Valley, CA.
29. Freire, E. (1998) *Adv. Protein Chem. 51*, 255−279.
30. Lakowicz, J. R. (1999) *Principles of Fluorescence Spectroscopy*, 2nd ed., Kluwer Academic/Plenum Publishers, New York.
31. Runnels, L. S., and Scarlatta, S. F. (1995) *Biophys. J. 69*, 1569−1583.
32. Pettigrew, D. W. (1986) *Biochemistry 25*, 4711−4718.
33. Hurley, J. H. (1996) *Annu. Rev. Biophys. Biomol. Struct. 25*, 137−162.
34. Mills, F. C., Johnson, M. L., and Ackers, G. K. (1976) *Biochemistry 15*, 5350−5362.

BI027142L